European Scholar Journal (ESJ)
Available Online at: https://www.scholarzest.com
Vol. 3 No.5, May 2022
ISSN: 2660-5562

MODELING AND COMPARISON OF CLOSED-LOOP AND OPEN-LOOP ADAPTIVE OPTICS SYSTEMS

Mahmood K. Mirdan
Department of Astronomy and Space, College of science, University of Baghdad.
mahmood.merdan1107@sc.uobaghdad.edu.iq
Raaid N. Hassan, Bushra Q. Al-Aboodi
Department of Astronomy and Space, College of science, University of Baghdad.

Article history:
Received: 4th March 2022
Accepted: 4th April 2022
Published: 10th May 2022

Abstract:
Astronomers have known since the invention of the telescope that atmospheric turbulence affects celestial images. So, in order to compensate for the atmospheric aberrations of the observed wavefront, an Adaptive Optics (AO) system has been introduced. The AO can be arranged into two systems: closed-loop and open-loop systems. The aim of this paper is to model and compare the performance of both AO loop systems by using one of the most recent Adaptive Optics simulation tools, the Objected-Oriented Matlab Adaptive Optics (OOMAO). Then assess the performance of closed and open loop systems by their capabilities to compensate for wavefront aberrations and improve image quality, also their effect by the observed optical bands (near-infrared band and visible band), the shape of the telescope aperture (circular and hexagonal) and the atmospheric seeing conditions. The results showed that open-loop systems perform better than closed-loop systems at good seeing and vice versa. Also showed that closed-loop provides stability in the correction process over time, while the open-loop is a faster phase compensator.

Keywords: Adaptive Optics; Closed-Loop; Open-Loop; OOMAO.

1. INTRODUCTION

Adaptive Optics (AO) is a technique for keeping light concentrated when it goes out of focus. Every sighted person understands when something is out of focus; the image is fuzzy rather than clear and sharp. If the detected light is out of focus, it can either move to a better place where the light is in focus or apply a correction to bring the beam into focus without moving. This is a rule that our eyes follow on a regular basis. The adaptive process of focus sensing is a learned process, and the correction is a learned response. When the correction approaches its biophysical limit, it will require assistance from the outside in the form of corrective lenses. Our eyes are constantly adjusting due to a closed loop adaptive process involving optics. It is therefore called Adaptive Optics [1].

AO technology has been used in astronomical observations [2], retinal imaging [3], laser beam shaping [4] and other fields [5-7]. An AO system is composed of three major elements, a wavefront corrector, a wavefront sensor, and a control system. Depending on the sequence in which these components are arranged, two AO arrangements are found; they are the closed-loop and open-loop arrangements.

Since, most of the AO components operate in a closed feedback loop, the wavefront corrector (Deformable Mirror DM) first corrects for the incoming wavefront aberrations. After that, a portion of the light is redirected toward the Wavefront Sensor (WFS) in order to estimate the remaining aberrations that need to be corrected. The WFS signals are used by the control system to update the command signals sent to the wavefront corrector. As the incoming wavefront changes, these processes are performed constantly. [8].

The necessity for a 'guide' source to perceive the wavefront is a critical feature of AO; bright point sources perform best. Fortunately, the sky offers astronomers a plethora of point sources in the form of stars. They are, however, quite faint. Observations are now confined to the neighborhood of the brightest stars, which is only a small percentage of the sky. Extended, but ideally small, sources can also be used for wavefront

sensing if they are bright enough. This comprises not just solar system objects like asteroids and planet satellites, but also a few galaxy cores. [9–10].

2. MODELING METHODOLOGY

Simulation is essential for the development of any AO system since it allows designers to set the parameters of the AO components, troubleshoot the system, and even evaluate the efficiency of a system on a specific instrument. For these reasons, a variety of tools have been created and programmed in various modeling programs in order to offer conclusive answers for all AO systems.

Some of the modeling tools are Code for Adaptive Optics Systems (CAOS); it is a software application that allows a quick study of all the modules in a conventional AO system, enabling quick learning of all modules. It enables any AO user, beginner or expert, to fully comprehend the parameters that control all AO modules, from the creation of the atmospheric turbulent volume to the projection and correction by the DM [11]. A second tool is Yao, which stands for Yorick Adaptive Optics, which is an open-source AO software simulation package, which has been used to simulate medium-size AO systems for extremely large telescopes [12]. It is fast, flexible and an open source library on Github [13] where installation is supported on Linux and OsX.

In this paper, Objected-Oriented Matlab Adaptive Optics (OOMAO) has been utilized, which is a Matlab toolbox developed by Conan and Correia (2014) with the goal of modeling the behavior of an entire AO system [14]. OOMAO is designed fully in the Matlab programming language and employs various Matlab-built algorithms that have been written and optimized in packages of code. OOMAO's Matlab source code is freely available to download at the Github website [15].

As the title implies, the package is designed in an object-oriented style. Object-Oriented Programming or OOP is a contemporary programming language that allows for the easy and manageable building of huge and complex software architectures. OOP is a programming paradigm that focuses on objects and data rather than actions and logic, a classic procedural program is designed to take in input data, process it, and output results. [16]. OOMAO contains a large theoretical expression library for evaluating the statistical features of turbulence wavefronts.

2.1 Closed-Loop System

In the closed-loop or feedback configuration, most AO systems utilize this technique. The main difference between a closed-loop and an open-loop system is that the DM is placed before the beam splitter, compensating for wavefront aberrations on the incoming beam before it is sampled and recorded by the Shack-Hartmann WFS (SH-WFS).

As a result, the SH-WFS only detect the wavefront residual error. That is, the difference between the current incoming wavefront and the DM's last correction. This error is determined in order to update the DM's control signals. One of the advantages of closed-loop systems is that they have a high gain, which reduces wavefront error at the wavefront sensor input. As a result, any errors in the projected gain value can cause bias in the AO correction, which will compound as a residual error if not detected. A closed loop will be able to detect and compensate for this increasing residual error.

In order to model a closed-loop Adaptive Optics system using the OOMAO toolbox, the atmosphere must be defined first as it is composed of three turbulent layers with Fried coherent parameter r_0 of (10 and 20)cm and a 30m outer scale. The closed-loop system used one Natural Guide Star (NGS) on axis. Observed at two different wavelength bands (visible band V = 0.550μm and near infrared band J = 1.215μm) the wavefront will be sensed by using a 202 lenslet array sampled with a 100×100 pixels camera. Lenslets with less than 75% of the light of a fully illuminated lenslet are neglected, while the DM is constructed using a 212 actuator array powered by a monotonic influence function mechanically coupled at 50%. The telescope is modeled in two aperture shapes (circular and hexagonal) of 8m in diameter (D/r_0 = 40) with a 1 arcmin field of view (FoV). The phase screens' temporal evolution is sampled at 100Hz. The proposed closed-loop AO arrangement pattern for different parameters has been summarized in Figure (1).

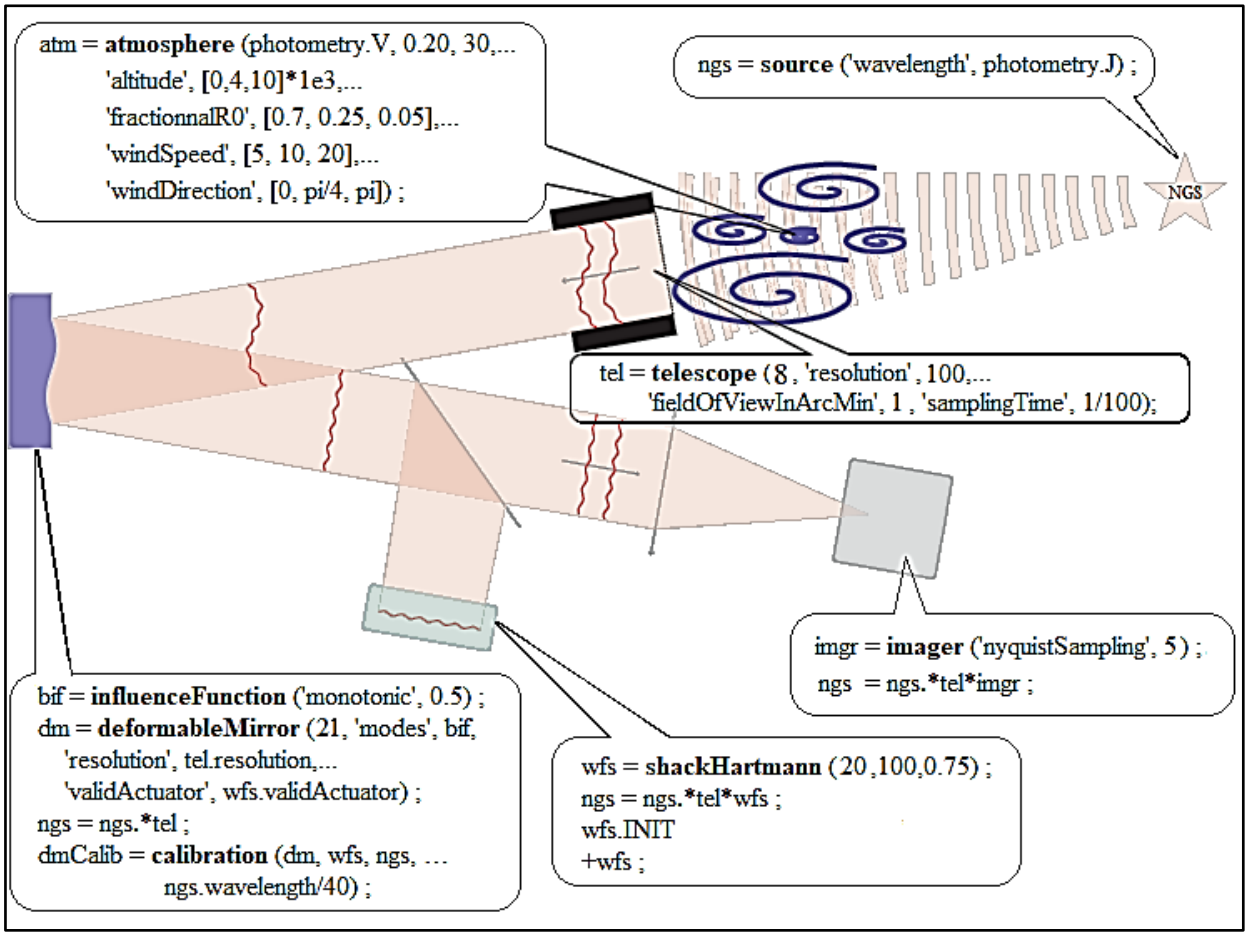

Figure 1. The proposed closed-loop AO arrangement.

2.2. Open-Loop System

In the open-loop or feed-forward configuration, a beam splitter is the first optical component in the path of light, as shown in Figure (2). This component divides the optical path into two. SH-WFS is used in the first path to fully measure the aberrations caused by the atmospheric turbulence. The measurement will be transmitted to a control computer, which will compute and send the required actuator commands to the DM. On the second path after the beam splitter, the commands will be applied by the DM, and the corrected beam will be transmitted to an imaging camera or any other scientific device that requires it.

Open-loop configurations have a few drawbacks, which result from the WFS's loss of the ability to see the DM. The first of these drawbacks is the inability to assess and map any distortions in the correction. WFSs and DMs are not all created equally. The second drawback is the presence of time-variant events that cannot be predicted in advance. They should instead be measured and corrected for in real time.

Despite their drawbacks, open-loop systems can be useful when trying to determine optical turbulence parameters from open-loop slopes, which are unaffected by the DM, or when there isn't a guiding star in the correction area of the sky.

The open-loop arrangement is the second AO system arrangement that has been simulated. In this section, the circular and hexagonal telescope apertures will be modeled and tested, but only the hexagonal form will be displayed in Figure (3). On the same approach of closed-loop system fulfillment, the open-loop has been implemented. The main difference here is the advance of SH-WFS over DM in the propagation optical

path as shown in Figure (2). The modeling is performed for the same classes' parameters in the closed-loop.

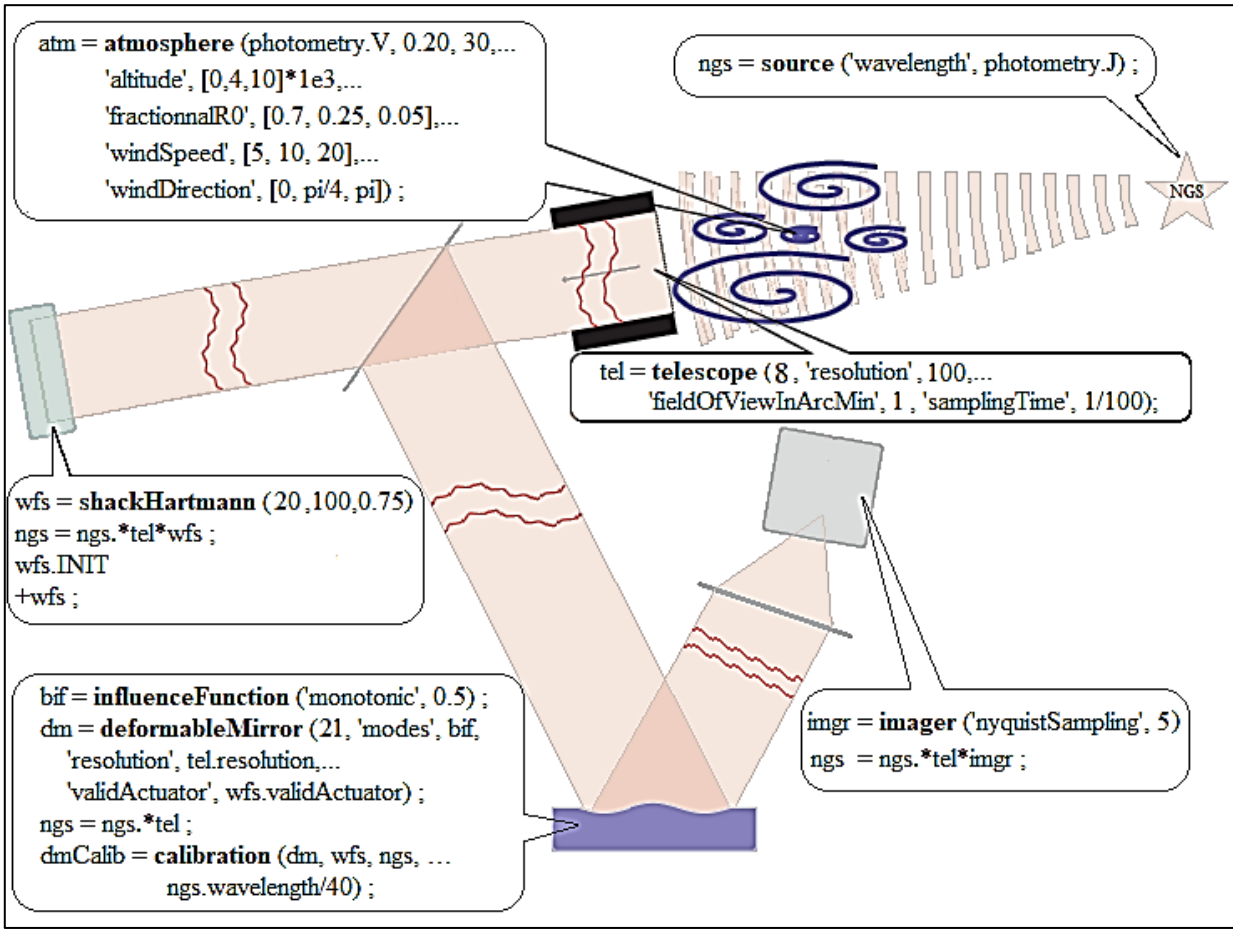

Figure 2. The proposed open-loop AO arrangement.

3. RESULTS AND DISCUSSION

In brief; both of the AO loop systems have been modeled in different cases, firstly: two telescope aperture shapes (circular and hexagonal), secondly: two observing wavelengths (visible band V = 0.550μm and near infrared band J = 1.215μm), thirdly: two seeing conditions at (r_0 = 10cm and 20cm). The simulation achieved by the means of OOMAO can be described briefly in the following sequence: creating the point source object and defining its location in the celestial sphere by azimuth and zenith (in this work the point source is on-axis NGS at 0 zenith and azimuth), furthermore, defining the observing wavelength band (in this work, V-band and J-band).

Next; create the atmosphere and define its turbulence layers with wind speed, direction and altitude then define the strength of that turbulence by the value of r_0. After that; create the telescope with the desired aperture diameter and shape. Subsequently; create the SH-WFS by defining the subapertures array (lenslets array) and then create the DM components, which are the actuators array and the type of influence function that powers the actuators up.

Once the DM components and the SH-WFS have been implemented, the Poke Matrix can be computed (the Poke Matrix is the interaction matrix between the SH-WFS and the DM), where it can be generated by pushing all the valid actuators consecutively and saving the corresponding SH-WFS slopes measurements in a matrix. This is done with the calibration method of the DM with SH-WFS (SH-WFS/DM calibration).

After that, in the closed-loop case, the NGS is propagated through the telescope reflected by DM to the SH-WFS {ngs = ngs.×tel×dm×wfs}, while in the open-loop case, the NGS is propagated through the telescope to the SH-WFS and DM in parallel form {ngs = ngs.×tel×wfs×dm}, then the SH-WFS saves the slopes corresponding to the 341 valid actuators for circular geometry and 271 valid actuators for hexagonal geometry (see Actuators Commands in Figure 3).

The source has been propagated through the DM as many times as the number of columns in the DM coefficients matrix. As a result, the slopes in the SH-WFS object are also a matrix; each column corresponds to one actuator. Slopes measurements in Figure 3) show the wavefront distortion measurements of the observed source when propagated through SH-WFS valid lenslets, where the distorted wavefront will form at a shifted XY coordinate (slopes) that forms the subaperture focus, while the non-distorted wavefront will form at the focus of the SH-WFS valid lenslet.

The moment that the Poke matrix has been determined, the DM's actuator command matrix can be derived. From the phase screen and command matrix, we can obtain the actuator commands. The command vector would be obtained by multiplying the measured slopes by the command matrix. These commands would be calculated at each step of the AO closed-loop by subtracting the measured slopes times the command matrix times the AO system gain from the last iteration (n) of calculated commands, while for open-loop these commands would be calculated from the opposite of the command matrix times the measured slopes.

At the beginning, the loop is closed for n = 100 time steps (i.e., 1 s) with an integrator gain of 0.5. While the second loop is closed for n=100 time steps with a detector read-out noise of about 5 photo-electrons per pixel per frame, it is good to mention that there is no gain in the open-loop system, since the DM compensates for the incoming aberrated wavefront in real-time, as opposed to the closed-loop where the DM compensates for the residual error from the last correction step.

Figure (3) shows the last step of the closed and open loop simulation, which is the wavefront compensation by DM reconstruction coefficients. Moreover, the loop has been applied to an aberrated image of an NGS source observed by circular and hexagonal telescopes. The outputs show to what extent it is possible to correct distortions in the image of the observed object, as shown in the compensation visualization in Figure (3).

The aberrated wavefront and its residual error accompanied by the DM reconstruction coefficients can be displayed particularly in an isometric shape as shown in Figure (4). Through both loops' procedure, a real time wavefront reconstruction is performed, targeting the phase of that wavefront in order to compensate for the aberrated wavefront and get the lowest residual error possible. This is done by means of DM coefficients (DM shape), which deform the mirror surface into an inverted shape of the aberrated wavefront shape, and because of the non-perfect fitting of the DM shape with the aberrated wavefront shape, will lead to the aberrations are not fully compensated, which is normal in this field because there is no AO system that has 100% compensation capability. The remains of the aberration are called residual error (Figure 4).

The performance comparison between the closed and open loop systems achieved for the fidelity criteria (root mean square error RMSE and Strehl ratio SR) for two different aperture shapes (circular and hexagonal), two wavelength bands (near-infrared J-band and visible V-band) and two different conditions seeing (r_0 = 10cm and 20cm), SR and RMSE are computed from the phase variance of the aberrated and compensated wavefront. This was completed in two cases with and without read-out noise.
Overall, the calculation outcomes will be four vector rows for both SR and RMSE, where the phase of the aberrated and compensated wavefronts will be referred to as 'Full Turbulent' and 'Residue Turbulent' respectively; while for the noise case the term (noise) is added to the labels, i.e., 'Full Turbulent' means AO off and 'Residue Turbulent' means AO on. It's good to mention that higher SR and lower RMSE are desired. The performance comparison criteria are shown in Table (1).

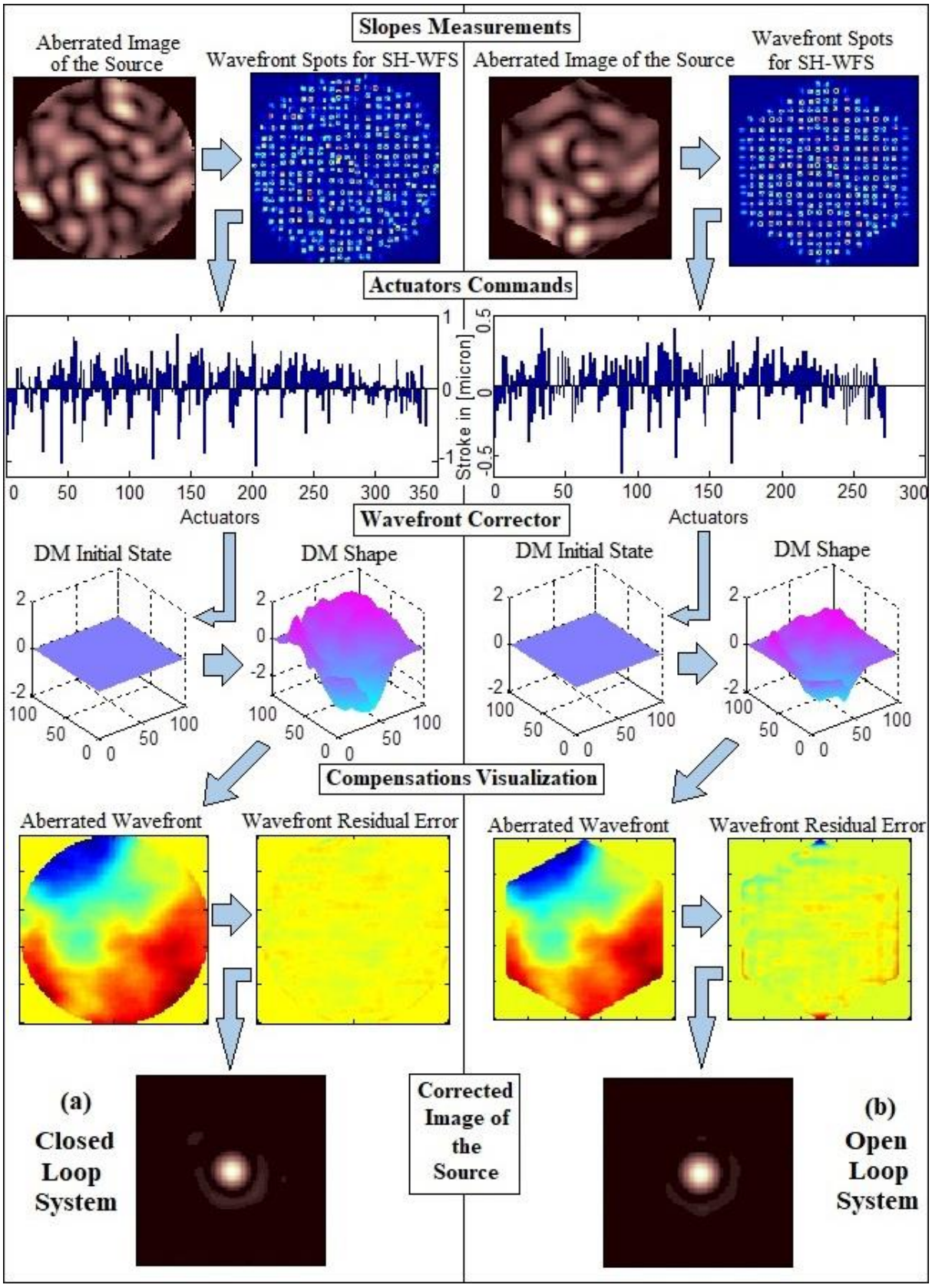

Figure 3. Wavefront compensation process flow in (a) Closed-loop system (b) Open-loop system.

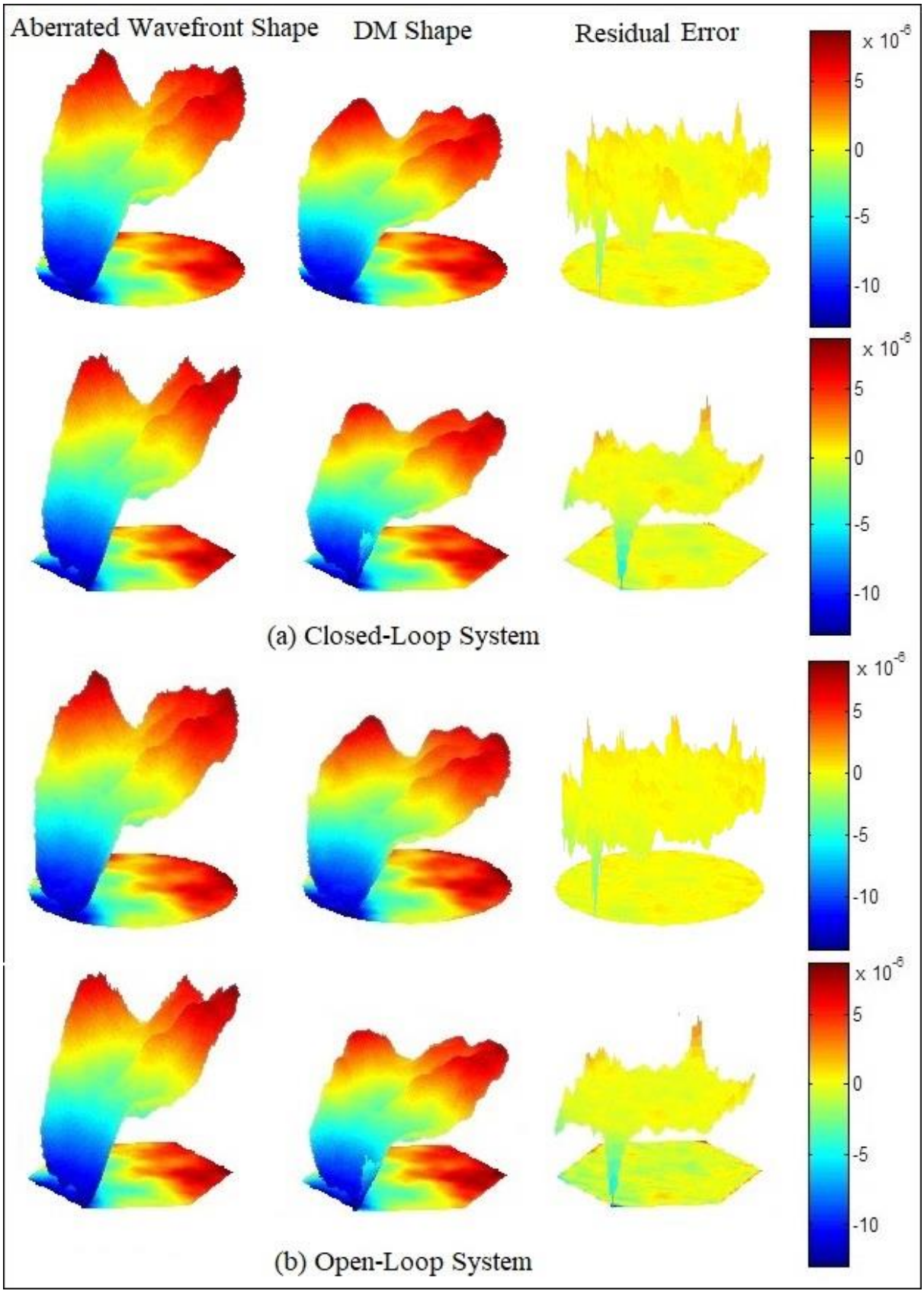

Figure 4. Wavefront compensation by DM reconstruction coefficients in (a) Closed-Loop System (b) Open-Loop System.

Table 1. The Performance Comparison Criteria of Closed and Open loop Systems.

Fidelity Criteria		RMSE (nm)				SR			
	Seeing	r_0 = 10cm		r_0 = 20cm		r_0 = 10cm		r_0 = 20cm	
	Aperture	Cir.	Hex.	Cir.	Hex.	Cir.	Hex.	Cir.	Hex.
Near-Infrared band J = 1.215µm	System	*Closed - Loop System*							
	Full Turbulent	1363	1297	765	728	7×10^{-19}	2×10^{-16}	8×10^{-7}	5×10^{-6}
	Full (Noise)	1705	1589	957	892	4×10^{-24}	4×10^{-20}	6×10^{-9}	9×10^{-8}
	Residual Turbulent	174	195	95	107	0.45	0.37	0.79	0.73
	Residual (Noise)	155	181	89	103	0.53	0.42	0.81	0.75
	System	*Open - Loop System*							
	Full Turbulent	1363	1297	765	728	9×10^{-86}	9×10^{-86}	3×10^{-28}	2×10^{-24}
	Full (Noise)	1705	1589	957	892	10^{-99}	10^{-99}	8×10^{-36}	9×10^{-30}
	Residual Turbulent	218	238	100	112	0.01	0	0.28	0.21
	Residual (Noise)	168	191	86	101	0.04	0.01	0.38	0.27
Visible band V = 0.550µm	System	*Closed - Loop System*							
	Full Turbulent	1363	1297	765	728	7×10^{-19}	2×10^{-16}	9×10^{-7}	5×10^{-6}
	Full (Noise)	1705	1589	957	892	5×10^{-24}	3×10^{-20}	6×10^{-9}	9×10^{-8}
	Residual Turbulent	236	248	81	96	0.26	0.23	0.84	0.78
	Residual (Noise)	189	205	76	93	0.39	0.33	0.86	0.79
	System	*Open - Loop System*							
	Full Turbulent	1363	1297	765	728	9×10^{-86}	4×10^{-74}	3×10^{-28}	2×10^{-24}
	Full (Noise)	1705	1589	957	892	4×10^{-99}	2×10^{-16}	9×10^{-36}	9×10^{-30}
	Residual Turbulent	718	682	178	179	0	0	0.04	0.04
	Residual (Noise)	721	653	151	150	0	0	0.06	0.06

The results in Table (1) demonstrate that both AO systems are capable of compensating the phase of the source aberrated wavefront with good accuracy (in the case of near-infrared J-band accuracy average > 80% represented by RMSE) but with slight differences in residual error between these systems, where in J-band at good seeing (r0 = 20cm), the open-loop has better accuracy than the closed-loop by 14% and 10% for circular and hexagonal apertures, respectively. While at indifferent seeing (r0 = 10cm), the closed-loop now has better accuracy than the open-loop by about 18% and 12% for circular and hexagonal apertures, respectively.

Either in the case of V-band at good seeing, the closed-loop has better accuracy than the open-loop by 43% and 33% for circular and hexagonal apertures, respectively, and at indifferent seeing, the closed-loop still has better accuracy of about 77% and 70% for circular and hexagonal apertures, respectively.

In addition; the results showed that both AO systems improve the image quality, especially at higher observing wavelengths (near-infrared band), where in the closed-loop the quality (represented by SR) has been improved by 53% and 81% at indifferent and good seeing conditions, respectively, for circular aperture, while for hexagonal aperture the quality improved by 42% and 75% at indifferent and good seeing conditions, respectively.

whereas in the open-loop, the quality of circular apertures improved by 39% and 86% at indifferent and good seeing conditions, respectively, while hexagonal apertures improved by 33% and 79% at indifferent

and good seeing conditions, respectively. The advantage between the two systems appeared at visible wavelengths, where the open-loop failed to improve the image quality for both seeing conditions, while the closed-loop was functional only at good seeing, where image resolution improved by 38% and 27% for circular and hexagonal apertures, respectively, while at indifferent seeing the closed-loop produced a pretty low resolution.

To clarify this comparison more, the two systems' performance have been displayed in Figure (5), which was conducted by a circular telescope aperture for near-infrared observing wavelength (J-band) at two seeing conditions. Figure (5) illustrates that the open-loop system performs better than the closed-loop at good seeing and vice versa, as well as in the correction process starts; the open-loop reaches its maximum correction capability a bit faster than the closed-loop, where the closed-loop is delayed by about 50 milliseconds. Despite all of the above, the closed loop system has proven the correction process stability over time, regardless of good or indifferent seeing conditions.

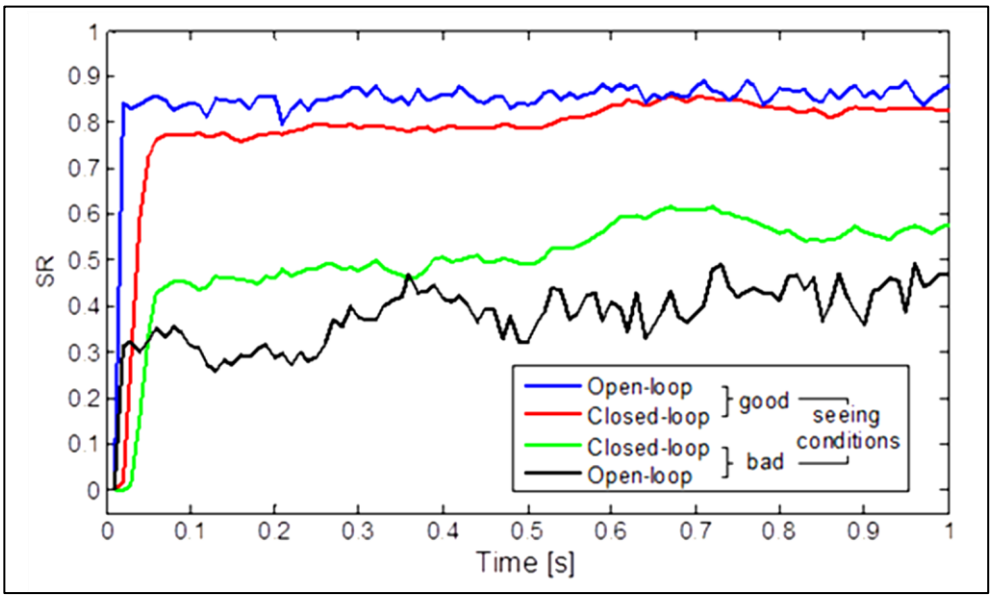

Figure 5. Open-Loop and Closed-Loop Performance Comparison for Circular Aperture.

4. CONCLUSIONS

From the results presented in this work, some remarks related to the modeling and comparison performance between Closed-Loop and Open-Loop AO systems were reported. Some of the important conclusions could be presented as follows:

- At longer optical wavelengths, both systems showed high accuracy in phase compensation by about (> 80%). Whereas in shorter optical wavelengths, the closed-loop is preferred because it outperforms the open-loop in this observing band (V-band), especially under poor seeing conditions.
- The AO closed-loop system provides the lowest residual error throughout the compensation process when compared to the open-loop system on all scales.
- The strength of the atmospheric turbulence and seeing conditions negatively affect the image quality. So in order to get the best astronomical observations, the open-loop system could be used for good seeing conditions ($r_0 \geq 20$cm) and the closed-loop system for indifferent seeing ($r_0 < 20$cm). This is because this simulation showed that the open-loop system performs better than the closed-loop at good seeing and vice versa.
- An open-loop system is a bit faster than a closed-loop system in wavefront phase compensation.
- The fluctuations in the open-loop system led to its use for short-exposure imaging since it's a faster phase compensator, while the stability in the correction process over time in the closed-loop system makes it an excellent choice for long exposure imaging, regardless of seeing conditions.

- In all circumstances, the circular shape of the telescope aperture provides the best correction accuracy and image quality when compared to the hexagonal aperture shape. This is due to the low number of valid actuators (271 actuators) counted from DM's actuator map depending on hexagonal geometry compared to 341 actuators for circular geometry.

REFERENCES

1. R. Tyson, Principles of Adaptive Optics, 3rd ed., CRC Press, Florida, 2010.
2. S. Maji, H. Yahia, T. Fusco, A Multifractal-based wavefront phase estimation technique for ground-based astronomical observations. *IEEE Trans. Geosci. Remote Sens.,* vol. 54, no. 3, pp. 1705-1715, 2016. https://doi.org/10.1109/TGRS.2015.2487546.
3. S. Niu, J. Shen, C. Liang, Y. Zhang, B. Li, High-resolution retinal imaging with micro adaptive optics system. *Appl. Opt.*, vol. 50, no. 22, pp. 4365-4375, 2011. https://doi.org/10.1364/AO.50.004365.
4. H. Ma, Z. Liu, X. Xu, J. Chen, Simultaneous adaptive control of dual deformable mirrors for full-field beam shaping with the improved stochastic parallel gradient descent algorithm. *Opt. Lett.*, vol. 38, no. 3, pp. 326-328, 2013. https://doi.org/10.1364/OL.38.000326.
5. R. Bastaits, D. Alaluf, M. Horodinca, I. Romanescu, I. Burda, G. Martic, G. Rodrigues, A. Preumont, Segmented bimorph mirrors for adaptive optics: Segment design and experiment. *Appl. Opt.*, vol. 53, no. 29, pp. 6635-6642, 2014. https://doi.org/10.1364/AO.53.006635.
6. Bayanna, R. Louis, S. Chatterjee, S. Mathew, P. Venkatakrishnan, Membrane based deformable mirror: intrinsic aberrations and alignment issues. *Appl. Opt.*, vol. 54, no. 7, pp. 1727-1736, 2015. https://doi.org/10.1364/AO.54.001727.
7. H. Ma, P. Zhou, X. Wang, Y. Ma, F. Xi, X. Xu, Z. Liu, Near-diffraction-limited annular flattop beam shaping with dual phase only liquid crystal spatial light modulators, *Opt. Express*, vol. 18, no. 8, pp. 8251-8260, 2010. https://doi.org/10.1364/OE.18.008251.
8. R. Tyson, B. Frazier, Field Guide to Adaptive Optics, 2nd ed., SPIE Press, Washington, 2012.
9. J. Hardy, Adaptive Optics for Astronomical Telescopes. Oxford University Press 1998, New York, USA, 1998.
10. F. Roddier, Adaptive Optics in Astronomy, Cambridge CB2, United Kingdom, 1999.
11. M. Chebbo, B.L. Roux, J.F. Sauvage, T. Fusco, Simulation of wavefront measurement and tomography for Extremely Large Telescope, *Proc. of SPIE,* vol. 7736, pp. 77364G, 2010. https://doi.org/10.1117/12.856387.
12. F. Rigaut, M. van Dam, Simulating Astronomical Adaptive Optics Systems Using Yao, *Proceedings of the Third AO4ELT Conference*, (2013).
13. F. Rigaut, M. van Dam, J. Cranney, S. Hippler, Yao an Adaptive Optics Simulation Package, http://github.com/frigaut/yao. (Accessed January 3, 2022).
14. R. Conan, C. Correia, Object-Oriented Matlab Adaptive Optics Toolbox, *Proc. SPIE*, vol. 9148, pp. 91486C, 2014. https://doi.org/10.1117/12.2054470.
15. R. Conan, Object-Oriented Matlab and Adaptive Optics, https://github.com/rconan/OOMAO. (Accessed January 3, 2022).
16. Reeves, Laser Guide Star Only Adaptive Optics: The Development of Tools and Algorithms for the Determination of Laser Guide Star Tip-Tilt. Durham University, United Kingdom, (2015).